Conference materials
UDC 621.383.52
DOI: https://doi.org/10.18721/JPM.161.312

Investigation of infrared photoresponse from structure with GeSiSn/Si multiple quantum wells

V.A. Timofeev [1]✉, V.I. Mashanov [1], A.I. Nikiforo[v] [1], I.V. Skvortsov [1],
A.A. Bloshkin [1], I.D. Loshkarev [1], I.A. Azarov [1], V.V. Kirienko [1]

[1] A.V. Rzhanov Institute of Semiconductor Physics SB RAS, Novosibirsk, Russia
✉ Vyacheslav.t@isp.nsc.ru

Abstract. The current-voltage (I-V) characteristics and spectral dependences of the photocurrent of *p-i-n* structures, including GeSiSn/Si multiple quantum wells (MQWs) with the Sn content up to 15%, are studied. It is shown that the increase in the Sn content from 4.5 to 13% leads to a gradual increase in the dark current density from 6×10^{-6} A/cm^2 to 5×10^{-5} A/cm^2 at the reverse bias of 1 V. The further rise in the Sn content to 15% results in the increase of the dark current density to 5×10^{-4} A/cm^2, which is an order of magnitude lower than the known values for GeSn-based photodiodes. The shift of the cutoff wavelength of the photoresponse with the Sn content increase in heterostructures is demonstrated. The photoresponse spectrum of the detector extends up to wavelengths of larger than 2 μm at the Sn content of more than 10%.

Keywords: multiple quantum well, band diagram, dark current, photocurrent

Funding: This work was supported by the Russian Science Foundation (RSF), Grant No. 20-79-10092.

Citation: Timofeev V.A., Mashanov V.I., Nikiforov A.I., Skvortsov I.V., Bloshkin A.A., Loshkarev I.D., Azarov I.A., Kirienko V.V., Investigation of infrared photoresponse from structure with GeSiSn/Si multiple quantum wells St, Petersburg State Polytechnical University Journal. Physics and Mathematics. 16 (1.1) (2023) 73–78. DOI: https://doi.org/10.18721/JPM.161.312

Материалы конференции
УДК 621.383.52
DOI: https://doi.org/10.18721/JPM.161.312

Исследование инфракрасного фотоотклика от структуры с множественными квантовыми ямами GeSiSn/Si

В.А. Тимофеев [1]✉, В.И. Машанов [1], А.И. Никифоров [1], И.В. Скворцов [1],
А.А. Блошкин [1], И.Д. Лошкарев [1], И.А. Азаров [1], В.В. Кириенко [1]

[1] Институт физики полупроводников им. А. В. Ржанова СО РАН, Новосибирск, Россия
✉ Vyacheslav.t@isp.nsc.ru

Аннотация. Исследованы вольт-амперные характеристики и спектральные зависимости фототока *p-i-n* структур, включающих множественные квантовые ямы GeSiSn/Si с содержанием Sn вплоть до 15%. Показано, что увеличение содержания олова от 4.5 до 15% приводит к увеличению плотности темнового тока с 6×10^{-6} А/см^2 до 5×10^{-4} А/см^2 при обратном смещении 1 В. Продемонстрировано, что увеличение содержания олова в гетероструктурах приводит к увеличению длинноволновой границы фотоответа вплоть до 2.25 μm.

Ключевые слова: множественная квантовая яма, зонная диаграмма, темновой ток, фототок

Финансирование: Работа выполнена при поддержке Российского научного фонда (РНФ), грант № 20-79-10092.

Ссылка при цитировании: Тимофеев В.А., Машанов В.И., Никифоров А.И., Скворцов И.В., Блошкин А.А., Лошкарев И.Д., Азаров И.А., Кириенко В.В. Исследование инфракрасного фотоотклика от структуры с множественными квантовыми ямами GeSiSn/Si // Научно-технические ведомости СПбГПУ. Физико-математические науки. 2023. Т. 16. № 1.1. С. 73–78. DOI: https://doi.org/10.18721/ JPM.161.312

Introduction

The new class of Ge-Si-Sn materials demonstrates promise for creating infrared photodetectors with the operation wavelengths from 1.55 up to 8 μm [1–3]. This range represents the best option for remote reading and the visualization of information due to reduced Rayleigh scattering and due to the transparency windows of the Earth's atmosphere near 1.6 μm, 3–5 μm and 8–14 μm. Infrared photodetectors based on GeSiSn are of great importance in applications ranging from fiber-optic communications to thermal imaging. Since Sn is the isovalent element with respect to Ge and Si, and also has the diamond-like crystal structure, photodetectors based on new GeSiSn materials will be able to compete with the group II-VI (HgCdTe)-based photodetectors due to better compatibility of the material with the existing Si technology.

Nowadays, there are many publications related to the GeSiSn-based photodetectors with the indication of their electrophysical parameters, such as the dark current, responsivity and cutoff wavelength [4, 5]. These parameters were included in tables presented in contributions [6, 7]. The dark current magnitude determines the signal-to-noise-ratio of the photodetectors, therefore it should be minimized. The lowest reported value of the dark current around 6×10^{-3} A/cm^2 was achieved for $Ge_{0.964}Sn_{0.036}$-based photodiodes [8]. The dark current has two components, namely: bulk and surface leakage currents. The first part is directly associated with the number of dislocations [9], whereas the second contribution is related to the surface defects of the mesa sidewall region. The later may be suppressed by the sidewall surface passivation [10].

The most photodiode structures grown on the Si substrate contain relaxed GeSn layers on the Ge layer. The GeSn and Ge layer thickness can reach several hundred nanometers. Due to the large lattice parameter mismatch between GeSn, Ge and Si, the dislocations are introduced. These defects increase the dark current of the photodiode. The issue may be solved by the application of the elastic strained layers. In this article such elastic strained (pseudomorphic) layers were used in the GeSiSn/Si multiple quantum well structures (MQW), which were embedded in the active region of the *p-i-n* diode. The lowest dark current density value in the GeSiSn/Si MQW diodes was about 6×10^{-6} A/cm^2. This dark current density is three orders of magnitude smaller than one of literature.

Materials and Methods

To study the photoelectric properties of structures with GeSiSn/Si MQWs, a series of samples with different tin content was grown. All samples were obtained on p^+-Si substrates. The 200 nm thick buffer layer was formed on the Si surface. After the growth of the buffer layer an active region was grown. It consisted of ten $Ge_{0.3}Si_{0.7-y}Sn_y$ quantum wells of the 2 nm thickness, which were separated by 7 nm thick Si layers. The Sn content in the samples varied from 3.5 to 15%. Further, the 100 nm thick undoped Si layer and the 50 nm thick n+-Si layer were grown. The *p-i-n* diodes in the form of mesa-structures with the diameter of 1.7 mm were fabricated using standard technological processes such as optical lithography, plasma etching and metal deposition in vacuum. The etching was performed down to the Si substrate. Au/Ti layers deposited in a high-vacuum setup were used to create ring electrodes to the heavily doped n^+-Si layers. The schematic photodetector structure is shown in Fig.1, *a*. Before mounting detectors fabricated into a cryostat for photoelectric measurements, the current-voltage (I–V) characteristics of devices were

measured at room temperature. The compositions and quality of epitaxial structures were studied by X-ray diffractometry. The diffraction reflection curves were obtained using the symmetric two-crystal scheme with the DSO-1T diffractometer and the Ge(004) single-crystal monochromator. The photocurrent spectra were measured using a Bruker Vertex-70 infrared Fourier spectrometer. The samples were placed in the Janis cryostat and cooled to the temperature of 77 K with liquid nitrogen. The photocurrent was recorded using an SR570 low-noise preamplifier from Stanford Research System. A halogen lamp was used as a light source.

The calculation of the energy band diagrams of the Si/$Ge_{1-x-y}Si_xSn_y$/Si heterocomposition, including a pseudomorphic $Ge_{1-x-y}Si_xSn_y$ layer, was carried out using a model-solid theory, which makes it possible to take into account the effects of strain on the band structure [11]. The model parameters for the GeSiSn ternary compound were determined by a linear interpolation of data for Ge, Si, and Sn [12–14]. The band gaps of the solid solution were calculated by the quadratic interpolation:

$$E^{\xi}\left(Ge_{1-x-y}Si_xSn_y\right) = E^{\xi}(Ge)\cdot(1-x-y) + E^{\xi}(Si)\cdot(x) + E^{\xi}(Sn)\cdot(y) - \\ -b^{\xi}_{SiGe}\cdot(1-x-y)\cdot x - b^{\xi}_{GeSn}\cdot(1-x-y)\cdot y - b^{\xi}_{SiSn}\cdot x\cdot y, \quad (1)$$

where, E^{ξ}(Ge), E^{ξ}(Si) and E^{ξ}(Sn) are Ge, Si and Sn band gaps, respectively; b^{ξ}_{SiGe}, b^{ξ}_{GeSn} and b^{ξ}_{SiSn} correspond to the bowing parameters; index $\xi = \Gamma, L, X$ refers to the different conduction valleys [13]. The effects of confinement were taken into account using effective mass theory. The interpolation suggested in [15] was used to calculate the effective masses.

Results and Discussion

A series of *p-i-n* diodes including $Ge_{0.3}Si_{0.7-y}Sn_y$/Si MQWs was obtained. The pseudomorphic state of $Ge_{0.3}Si_{0.7-y}Sn_y$ layers was confirmed by the presence of diffraction peaks on the diffraction reflection curves (Fig. 1, *b*). Diffraction peaks are marked with integers from −3 to +1.

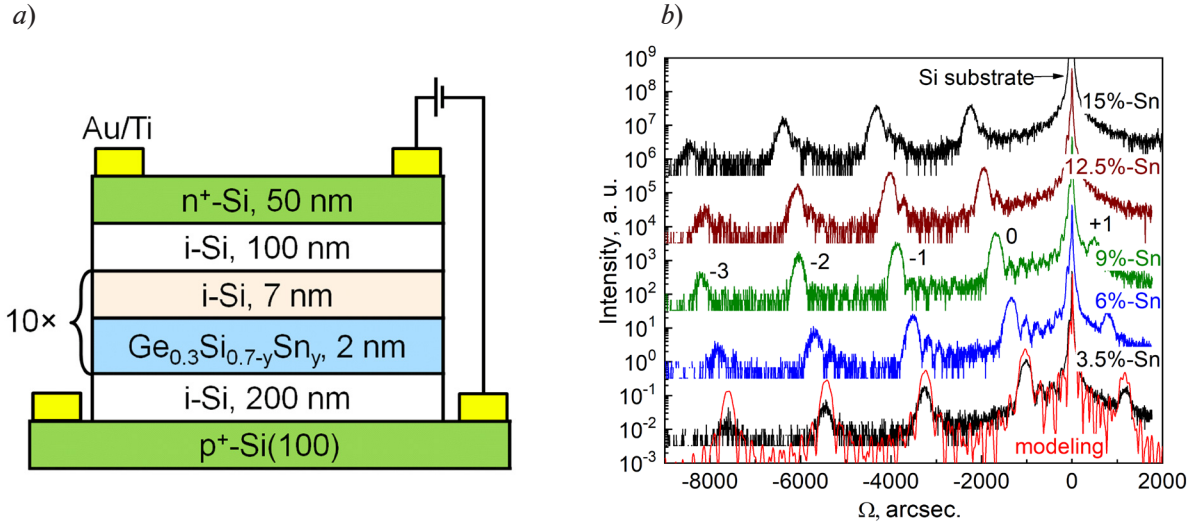

Fig. 1. Schematic cross section of a *p-i-n* diode with the $Ge_{0.3}Si_{0.7-y}Sn_y$/Si MQWs (*a*) and the (004) diffraction reflection curves from the MQWs containing 10 periods with the pseudomorphic $Ge_{0.3}Si_{0.7-y}Sn_y$ films for different Sn contents (*b*). The peak from the Si substrate is indicated by the arrow and the diffraction maxima are pointed out by the integers from −3 to +1

The distance between the satellites corresponds to the period in MQWs. The average composition was determined from the distance between the zero satellite and the peak from the Si substrate. The shift of the zero satellite is observed with the Sn content increase from 3.5 to 15%. The rocking curves were simulated taking into account the pseudomorphic state of the $Ge_{0.3}Si_{0.7-y}Sn_y$ layers. The modeling curve for the Sn content of 3.5% is shown as the example. It is in good agreement with the experimental dependence for the same composition.

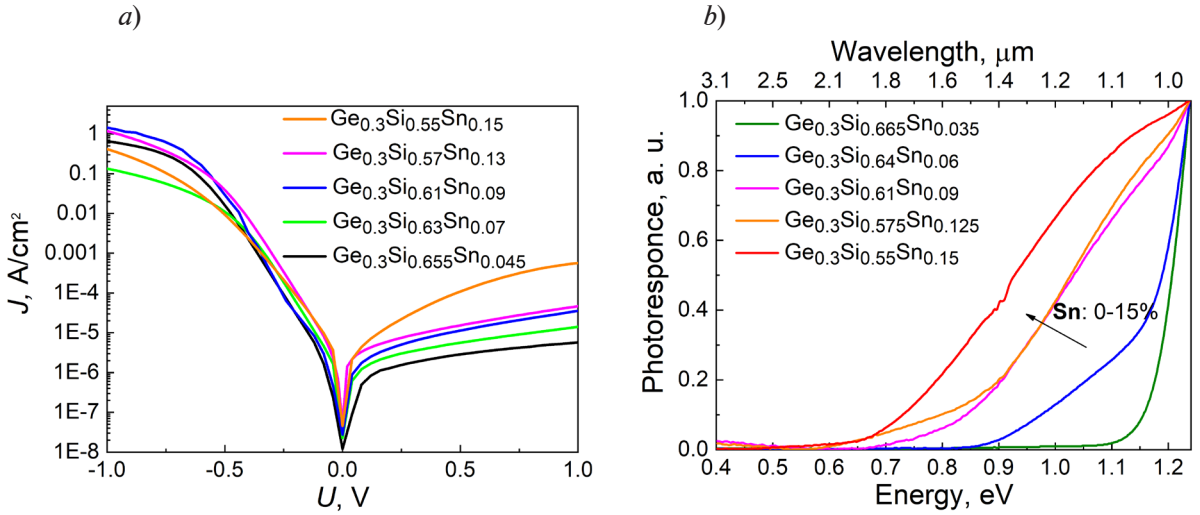

Fig. 2. Dark current-voltage (I–V) characteristics of p-i-n diodes for different Sn contents in GeSiSn quantum wells (*a*), photocurrent spectra of p-i-n diodes measured in short circuit regime at zero bias (*b*)

Based on the measurements of I–V characteristics and photocurrent spectra the photoelectric properties of p-i-n diodes obtained were studied. The I–V characteristics for samples containing up to 15% tin in quantum wells are shown in Fig. 2, *a*. All devices had diode I–V characteristics. It is shown that the increase in the Sn content from 4.5 to 13% leads to a gradual increase in the dark current density from 6×10^{-6} A/cm^2 to 5×10^{-5} A/cm^2 at a reverse bias of 1 V. The further rise in the Sn content to 15% results in the increase of the dark current density to 5×10^{-4} A/cm^2. The increase of the dark current density can be associated with the Sn segregation on the surface. It is confirmed by the appearance of the two-domain (4×1) superstructure during the growth on the reflection high energy electron diffraction pattern (RHEED). Such superstructure corresponds to the submonolayer Sn cover on the Si surface. The Sn segregation probably causes the surface leakage current increase on the sidewall surface of the mesa [10]. Despite the absence of the passivation and optimization of p-i-n diode dimensions, we achieved record values of the dark current density, which are a thousand times lower than the dark current densities of GeSn-based diodes presented in the literature for approximately the same Sn content [8]. The photocurrent spectra for the Sn content from 3.5 to 15% are shown in Fig. 2, *b*. The spectra were normalized

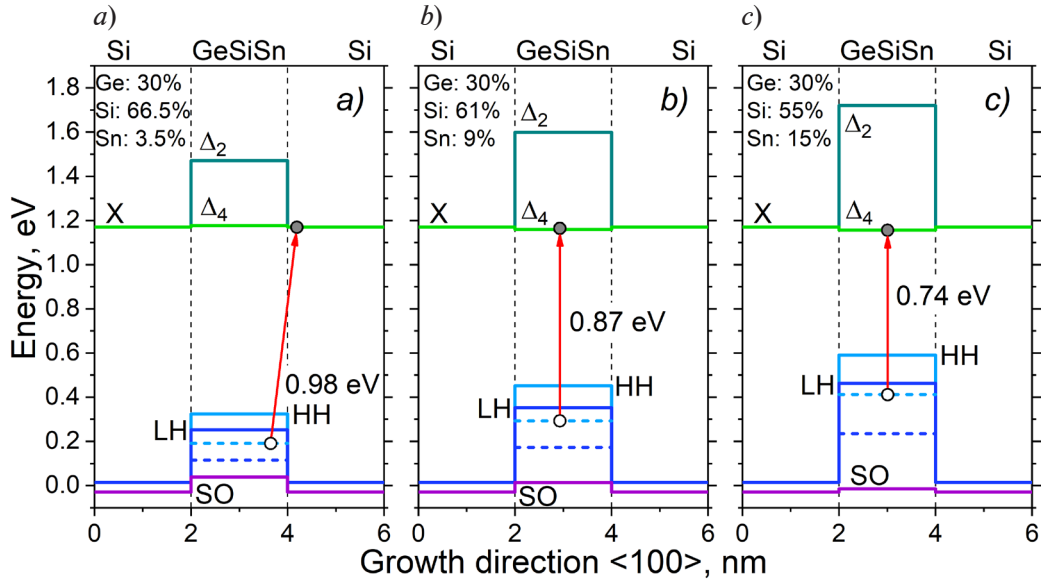

Fig. 3. Band diagrams for Si/$Ge_{0.3}Si_{0.7-y}Sn_y$/Si heterostructures with the Sn content of 3.5 (*a*), 9 (*b*) and 15% (*c*)

to the photocurrent maximum. For all samples, the large photoresponse signal with the energy near 1.2 eV is observed. This signal is associated with the interband optical transitions in silicon. The gradually decreasing photocurrent signal is observed with the photon energy decrease below the Si band gap. The cutoff wavelength of the photoresponse was determined by equating to zero of the first derivative of the photocurrent. The obtained values are presented in the inset in Fig. 2, *b*. The increase of the cutoff wavelength of the photoresponse from 1.18 to 2.25 μm is observed with the tin content increase from 3.5 to 15% in the $Ge_{0.3}Si_{0.7-y}Sn_y$ layers. According to band diagram calculations for $Si/Ge_{0.3}Si_{0.7-y}Sn_y/Si$ heterostructures (Fig. 3), the contribution to the photocurrent can occur from interband optical transitions between the valence band and X-valley in silicon, as well as transitions between subbands of heavy or light holes in the $Ge_{0.3}Si_{0.7-y}Sn_y$ solid solution layer and the X-valley in silicon or the Δ_4 subband in the $Ge_{0.3}Si_{0.7-y}Sn_y$ layer. The optical transitions with minimum energy are indicated by arrows in Fig. 3. However, the experimentally obtained values of the cutoff wavelength are lower than the calculated ones in terms of energy. This result can be explained by smearing of the GeSiSn/Si heterointerface. It is associated with the Sn segregation, which leads to a decrease in the optical transition energy.

Conclusion

A series of *p-i-n* diodes, including GeSiSn/Si MQWs with the Sn content up to 15%, was obtained. The gradual increase of the dark current density from 6×10^{-6} A/cm^2 to 5×10^{-5} A/cm^2 at the reverse bias of 1 V was observed with the Sn content increase from 4.5 to 13%. The further Sn content rise to 15% led to the dark current density increase up to 5×10^{-4} A/cm^2. However, these dark current densities are the smallest among those known from the literature for the GeSiSn/Si system. It was shown that the Sn content increase in heterostructures leads to the shift of the cutoff wavelength of the photoresponse up to 2.25 μm. Further investigation will be aimed at reducing the dark current by optimizing the size of the diode mesa and its sidewall passivation, as well as at increasing the cutoff wavelength of the spectral responsivity due to the higher Ge and Sn contents in the GeSiSn quantum wells.

Acknowledgments

This work was supported by the Russian Science Foundation (RSF), Grant No. 20-79-10092.

REFERENCES

1. **Chang C., Li H., Ku C.-T., Yang S.-G., Cheng H. H., Hendrickson J., Soref R. A., Sun G.,** $Ge_{0.975}Sn_{0.025}$ 320 × 256 imager chip for 1.6-1.9 μm infrared vision, Applied Optics. 55 (36) (2016) 10170–10173.

2. **Atalla M. R. M., Assali S., Attiaoui A., Lemieux-Leduc C., Kumar A., Abdi S., Moutanabbir O.,** All-Group IV Transferable Membrane Mid-Infrared Photodetectors, Advanced Functional Materials. 31 (3) (2020) 2006329.

3. **Xu C., Ringwala D., Wang D., Liu L., Poweleit C. D., Chang S. L. Y., Zhuang H. L., Menendez J., Kouvetakis J.,** Synthesis and Fundamental Studies of Si-Compatible (Si)GeSn and GeSn Mid-IR Systems with Ultrahigh Sn Contents, Chemistry of Materials. 31 (2019) 9831–9842.

4. **Su S., Cheng B., Xue C., Wang W., Cao Q., Xue H., Hu W., Zhang G., Zuo Y., Wang Q.,** GeSn *p-i-n* photodetector for all telecommunication bands detection, Optics Express. 19 (7) (2011) 6400.

5. **Xu S., Wang W., Huang Y.-C., Dong Y., Masudy-Panan S., Wang H., Gong X., Yeo Y.-C.,** High-speed photo detection at two-micron-wavelength: technology enablement by GeSn/Ge multiple-quantum-well photodiode on 300 mm Si substrate, Optics Express. 27 (4) (2019) 5798.

6. **Zheng J., Liu Z., Xue C., Li C., Zuo Y., Cheng B., Wang Q.,** Recent progress in GeSn growth and GeSn-based photonic devices, Journal of Semiconductors. 39 (6) (2018) 061006.

7. **Tran H., Pham T., Margetis J., Zhou Y., Dou W., Grant P. C., Grant J. M., Al-Kabi S., Sun G., Soref R. A., Tolle J., Zhang Y.-H., Du W., Li B., Mortazavi M., Yu S.-Q.,** Si-Based GeSn Photodetectors toward Mid-Infrared Imaging Applications, ACS Photonics. 6 (11) (2019) 2807–2815.

8. **Zhang D., Xue C., Cheng B., Su S., Liu Z., Zhang X., Zhang G., Li C., Wang Q.,** High-responsivity GeSn short-wave infrared *p-i-n* photodetectors, Applied Physics Letters. 102 (2013) 141111.

9. **Giovane L. M., Luan H.-C., Agarwal A. M., Kimerling L. C.,** Correlation between leakage current density and threading dislocation density in SiGe p-i-n diodes grown on relaxed graded buffer layers, Applied Physics Letters. 78 (4) (2001) 541–543.

10. **Dong Y., Wang W., Lei D., Gong X., Zhou Q., Lee S. Y., Loke W. K., Yoon S.-F., Tok E. S., Liang G., Yeo Y.-C.,** Suppression of dark current in germanium-tin on silicon *p-i-n* photodiode by a silicon surface passivation technique, Optics Express. 23 (14) (2015) 18611.

11. **Chris G. Van de Walle,** Band lineups and deformation potentials in the model-solid theory, Phys. Rev. B. 39 (1989) 1871–1883.

12. **El Kurdi M., Sauvage S., Fishman G., Boucaud P.,** Band-edge alignment of SiGe/Si quantum wells and SiGe/Si self-assembled island, Phys. Rev. B. 73 (2006) 195327.

13. **Moontragoon P., Soref R. A., Ikonic Z.,** The direct and indirect bandgaps of unstrained $Si_xGe_{1-x-y}Sn_y$ and their photonic device applications, J. Appl. Phys. 112 (2012) 073106.

14. **Attiaoui A., Moutanabbir O.,** Indirect-to-direct band gap transition in relaxed and strained $Ge_{1-x-y}Si_xSn_y$ ternary alloys, J. Appl. Phys. 116 (2014) 063712.

15. **Sant S., Schenk A.,** Pseudopotential calculations of strained-GeSn/SiGeSn hetero-structures, Appl. Phys. Lett. 105 (2014) 162101.

THE AUTHORS

TIMOFEEV Vyacheslav A.
Vyacheslav.t@isp.nsc.ru
ORCID: 0000-0003-4093-7802

BLOSHKIN Alexey A.
bloshkin@isp.nsc.ru
ORCID: 0000-0002-4128-6143

MASHANOV Vladimir I.
mash@isp.nsc.ru
ORCID: 0000-0003-4420-6695

LOSHKAREV Ivan D.
idl@isp.nsc.ru
ORCID: 0000-0003-4771-3705

NIKIFOROV Alexander I.
nikif@isp.nsc.ru
ORCID: 0000-0003-0583-0508

AZAROV Ivan A.
azarov_ivan@mail.ru
ORCID: 0000-0001-9571-2227

SKVORTSOV Ilya V.
i.skvortsov@isp.nsc.ru
ORCID: 0000-0002-2153-1615

KIRIENKO Viktor V.
victor@isp.nsc.ru
ORCID: 0000-0002-8842-5323

Received 29.11.2022. Approved after reviewing 23.01.2023. Accepted 25.01.2023.